World Scientific
www.worldscientific.com

Neutral Silicon-Vacancy Color Center in Diamond: Cluster Simulation of Spatial and Hyperfine Characteristics

A. L. Pushkarchuk

Institute of Physical-Organic Chemistry, NASB
Surganova Str. 13, 220072 Minsk, Belarus
alexp51@bk.ru

S. A. Kuten*

Institute for Nuclear Problems, Belarusian State University
Bobruiskaya Str. 11, 220030 Minsk, Belarus
kut@inp.bsu.by

V. A. Pushkarchuk*

Belarusian State University of Informatics and Radioelectronics
P. Browka 6, 220013 Minsk, Belarus
vadim@nv-center.com

A. P. Nizovtsev*,† and S. Ya. Kilin*,‡

B. I. Stepanov Institute of Physics NASB
Nezavisimosti Ave. 68, 220072 Minsk, Belarus
†apniz@dragon.bas-net.by
‡kilin@dragon.bas-net.by

One of the most promising platforms to implement quantum technologies are coupled electron-nuclear spins in solids in which electrons can play a role of "fast" qubits, while nuclear spins can store quantum information for a very long time due to their exceptionally high isolation from the environment. The well-known representative of such systems is the "nitrogen-vacancy" (NV) center in diamond coupled by a hyperfine interaction to its intrinsic $^{14}N/^{15}N$ nuclear spin or to ^{13}C nuclear spins presenting in the diamond lattice. More recently, other paramagnetic color centers in diamond have been identified exhibiting even better characteristics in comparison to the NV center. Essential prerequisite for a high-fidelity spin manipulation in these systems with tailored control pulse sequences is a complete knowledge of hyperfine interactions. Development of this understanding for one of the new color centers in diamond, *viz.*, neutral "silicon-vacancy" (SiV^0) color center, is a primary goal of this paper, in which we are presenting

*Corresponding authors.

preliminary results of computer simulation of spatial and hyperfine characteristics of SiV^0 center in H-terminated clusters C$_{84}$[SiV^0]H$_{78}$ and C$_{128}$[SiV^0]H$_{98}$.

1. Introduction

Hybrid spin systems consisting of electronic spins (e-spins) of single paramagnetic color centers (PCCs) in diamond and neighbor nuclear spins (n-spins) of isotopic ^{13}C atoms are now widely used to implement numerous room-temperature applications in quantum information processing, quantum sensing and metrology (see, e.g., recent reviews[1–3]). In these systems, the ^{13}C n-spins with their excellent coherence times serve as quantum memories accessed via the more easily controllable e-spins of the PCCs. In some cases, optical transitions of the PCC electrons are strong enough opening an opportunity of their individual excitation by focussed laser radiation and obtaining fluorescence emitted by single PCC. The well-known representative of such systems is the "nitrogen-vacancy" (NV) center that possesses properties of optical alignment and spin-dependent fluorescence, allowing its initialization and readout even at room temperature.[3]

More recently, the other PCCs in diamond have been identified exhibiting even better characteristics in comparison to the NV center.[4] Vacancy-related group-IV-element color centers (SiV, GeV, SnV) have recently attracted a considerable attention.[4–6] The main advantage of these centers in comparison to the NV center is the fact that most of their fluorescence belongs to a narrow (~ 1 nm) zero-phonon line (ZPL), whereas for the NV center this fraction is only $\sim 4\%$. Owing to such practically monochromatic fluorescence of the centers, the generation of indistinguishable photons has been obtained.[7]

The ground and excited electronic states of the new color centers have fine structures, which allow their coherent manipulation by microwaves, as it was demonstrated for the negatively charged SiV$^-$ center ($S = 1/2$).[8] However, the center exhibits very short spin coherence time of 38 ns even at 4.5 K.[9] In contrast, the neutral center SiV^0 with ZPL at 1.31 eV (946 nm) and ground-state electronic spin $S = 1$ has much longer spin coherence time.[10] The center is associated with the KUL1 electron paramagnetic resonance (EPR) center[11,12]

with zero-field splitting $D = 942$ MHz and can be stable in boron-doped diamond samples.[10] Evidently, surrounding ^{13}C nuclear spins can be used as an additional resource for quantum memory. Here we are presenting the preliminary analysis of hyperfine interactions for the SiV^0 center in diamond.

2. Simulation and Results

The center properties were studied by simulating two H-terminated clusters C$_{84}$[SiV^0]H$_{78}$ and C$_{128}$[SiV^0]H$_{98}$ hosting SiV centers in their central parts as it is shown in Fig. 1. Calculations have been performed for neutral clusters in the triplet ground state ($S = 1$) using the density functional theory (DFT). To optimize the geometry of the clusters, we have used the ORCA software package (the DFT/UKS/PW91/RI/def2-SVP level of theory).

During structural relaxation, there was no potential barrier for the Si atom on a trajectory from the substitutional site to an interstitial one between the two lattice vacancies. As a result, the relaxed geometries of both clusters exhibited the D$_{3d}$ symmetry. The Si atom is located in the interstitial position and has six nearest-neighbor carbon atoms at near-equal distances of 2.025–2.026 Å from it.

Using DFT/UKS/PW91/RI/def2-SVP level of theory, we calculated distributions of the total spin density $n(r) = n_\uparrow(r) - n_\downarrow(r)$, where $n_\uparrow$ and $n_\downarrow$ are the electron densities with spin up ($\uparrow$) and down ($\downarrow$) orientation, respectively. Calculated isosurfaces of $n(r)$ at values of 0.01 and 0.001 are shown in Fig. 1 for the cluster C$_{128}$[SiV^0]H$_{98}$. The spin density is localized mainly at six equivalent C atoms being nearest neighbors of the Si atom. It is positive. In turn, at smaller values, the spin density is spread rather far from Si atom. Note the appearance of areas with negative spin density in this case.

Then, we calculated (using ORCA software package) the matrices $\boldsymbol{A}_{\mathbf{KL}}$ describing hyperfine interaction (hfi) of the electronic spin $S = 1$ of the SiV^0 center with the nuclear spin $I = 1/2$ of isotopic ^{29}Si nucleus of the center and, as well, with nuclear spins $I = 1/2$ of ^{13}C atom located in all possible
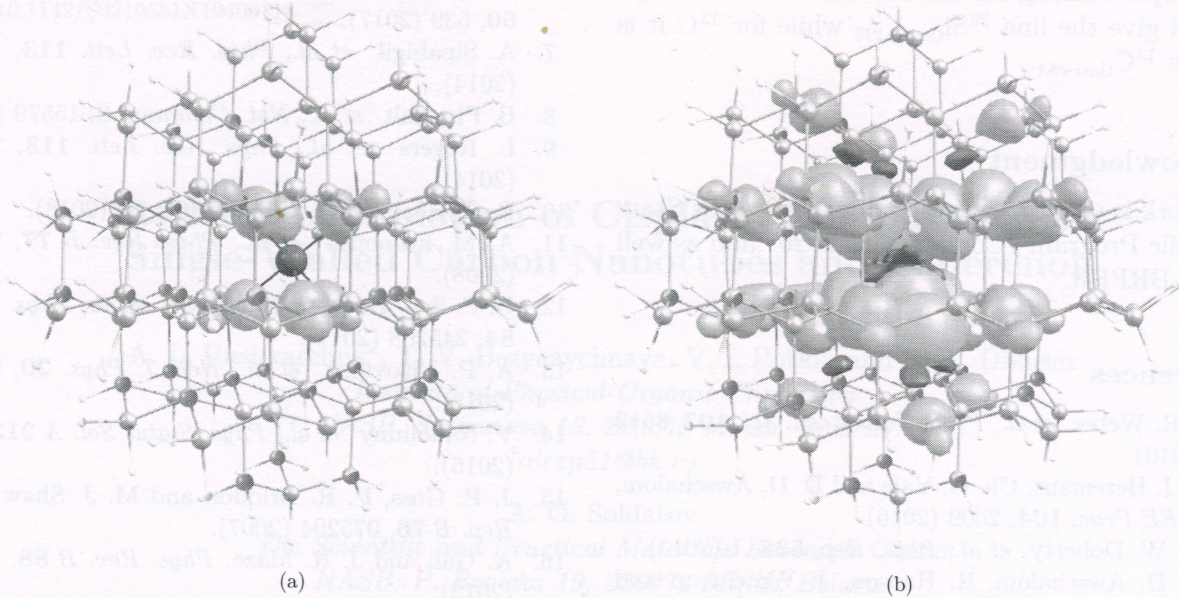
(a)   (b)

Fig. 1.   The relaxed $C_{128}[SiV^0]H_{98}$ cluster with shown isosurfaces of spin density equal to 0.01 (a) and 0.001 (b). Both figures are the side view with the (1 1 1) axis directed up in the plane of the figure. The ball in the cluster center is the Si atom. The lobes correspond to positive and negative spin densities. Passivating H atoms are shown at the cluster surface.

positions within the relaxed cluster. The calculations have been done in the coordinate system having the origin at Si atom and Z axis coinciding with (1 1 1) direction of the diamond lattice. Both isotropic and anisotropic contributions to the *hfi* matrices A_{KL} have been calculated. Using the matrices in the spin Hamiltonian of the center, we can calculate experimentally measured characteristics for various SiV^0–^{13}C spin systems (*hfi*-induced splitting of the $m_S = \pm 1$ substates, *hfi*-induced ^{13}C spin flip-flop rates, etc., see e.g., Ref. 13) in the cluster. These data will be published elsewhere. Here we confine ourselves to presenting the results for the ^{29}Si atom and for six nearest-neighbor ^{13}C atoms. These six atoms are near-equidistant from Si atom and have near-coinciding diagonalized *hfi* matrices.

In Table 1, we present the averaged values of the elements A_{xx}, A_{yy} and A_{zz} obtained by numerical diagonalization of *hfi* matrices A_{KL} calculated by ORCA using different levels of theory (UKS/PW91/RI/def2-SVP indicated as theo-a, UKS/B3LYP/G/3-21G indicated as theo-b, ROKS/PW91/RI/def2-SVP indicated as theo-c, numbers 84 and 128 represent $C_{84}[SiV^0]H_{78}$ and $C_{128}[SiV^0]H_{98}$ clusters, respectively). Note that in Ref. 15, *hfi* data (see lines $^{29}Si_{theo-Ref15}$ and $^{13}C_{theo-Ref15}$) have been obtained for 216-atom supercell using LDA-nocp without an account of the core polarization,

whereas in Ref. 16 (see lines $^{29}Si_{theo-Ref16}$, $^{13}C_{theo-Ref16}$) it has been done for 512-atom supercell using special HSE06-cp functional. It follows from Table 1 that in all simulations in agreement with the experiment, the *hfi* with ^{29}Si atom is almost isotropic, whereas the *hfi* with ^{13}C is

Table 1.   Comparison of experimental EPR hyperfine data of Refs. 11 and 14 (lines $^{29}Si_{exp}$, $^{13}C_{exp}$) with the calculated ones at different theory levels and in previous works Refs. 15 and 16 (lines, $^{29}Si_{theo-Ref15}$, $^{13}C_{theo-Ref15}$ and $^{29}Si_{theo-Ref16}$, $^{13}C_{theo-Ref16}$, respectively).

	A_{xx}	A_{yy}	A_{zz}
$^{29}Si_{exp}$	78.93	78.9	76.3
$^{29}Si_{theo-a84}$	58.3	60.6	60.6
$^{29}Si_{theo-b84}$	84.3	84.3	80.1
$^{29}Si_{theo-c84}$	−0.5	0.3	0.3
$^{29}Si_{theo-a128}$	54.5	57.4	57.4
$^{29}Si_{theo-b128}$	80.9	80.9	76.4
$^{29}Si_{theo-Ref15}$	82	82	78
$^{29}Si_{theo-Ref16}$	97	97	92
$^{13}C_{exp}$	30.2	30.2	66.2
$^{13}C_{theo-a84}$	51.6	51.6	86.5
$^{13}C_{theo-b84}$	44.0	44.1	77.1
$^{13}C_{theo-c84}$	25.9	26.0	57.3
$^{13}C_{theo-a128}$	51.9	51.9	86.4
$^{13}C_{theo-b128}$	44.5	44.6	77.5
$^{13}C_{theo-Ref15}$	12	12	51
$^{13}C_{theo-Ref16}$	28	28	68

anisotropic. Among our simulations, the best results for ^{29}Si give the line ^{29}Si$_{theo-b128}$ while for ^{13}C it is the line ^{13}C$_{theo-c84}$.

Acknowledgment

References

1. J. R. Weber *et al.*, *Proc. Natl. Acad. Sci.* **107**, 8513 (2010).
2. F. J. Heremans, Ch. G. Yale and D. D. Awschalom, *IEEE Proc.* **104**, 2009 (2016).
3. M. W. Doherty *et al.*, *Phys. Rep.* **528**, 1 (2013).
4. D. D. Awschalom, R. Hanson, J. Wrachtrup and B. B. Zhou, *Nat. Photon.* **12**, 518 (2018).
5. J. N. Becker and Ch. Becher, *Phys. Status Solidi A* **214**, 1700586 (2017).
6. E. A. Ekimov and M. V. Kondrin, *Phys.-Uspekhi* **60**, 539 (2017).
7. A. Sipahigil *et al.*, *Phys. Rev. Lett.* **113**, 113602 (2014).
8. B. Pingault *et al.*, *Nat. Commun.* **8**, 15579 (2017).
9. L. Rogers *et al.*, *Phys. Rev. Lett.* **113**, 263602 (2014).
10. B. C. Rose *et al.*, *Science* **361**, 60 (2018).
11. A. M. Edmonds *et al.*, *Phys. Rev. B* **77**, 245205 (2008).
12. U. F. S. D'Haenens-Johansson *et al.*, *Phys. Rev. B* **84**, 245208 (2011).
13. A. P. Nizovtsev *et al.*, *New J. Phys.* **20**, 023022 (2018).
14. V. Nadolinny *et al.*, *Phys. Status Sol. A* **213**, 2623 (2016).
15. J. P. Goss, P. R. Briddon and M. J. Shaw, *Phys. Rev. B* **76**, 075204 (2007).
16. A. Gali and J. R. Maze, *Phys. Rev. B* **88**, 235205 (2013).